

# Magnetic domain structure of colossal magnetoresistance thin films and islands

Trevor W. Olson

*Department of Physics, Cornell University, Ithaca, New York 14853*

Jeanine M. W. Olson

*Department of Materials Science and Engineering, University of California—Berkeley, Berkeley, California 94720*

Andreas Scholl

*Advanced Light Source, Lawrence Berkeley National Laboratory, Berkeley, California 94720*

Y. Suzuki

*Department of Materials Science and Engineering, University of California—Berkeley, Berkeley, California 94720*

(Presented on 9 January 2004)

We synthesized 10–200 nm thick colossal magnetoresistive  $\text{La}_{0.7}\text{Sr}_{0.3}\text{MnO}_3$  (LSMO) thin films under compressive strain, resulting in perpendicular anisotropy. Similar magnetic domain structures in LSMO films thicker than 40 nm were observed by magnetic force microscopy and were also seen with photoemission electron microscopy. Recent transport measurements, in conjunction with this result, suggest a dead layer at the interface, not at the surface. When varying the temperature from below the Curie temperature  $T_C$  to above, the magnetic domains disappeared. These domains nucleated uniformly across the film when the temperature was subsequently lowered, but their positions were unrelated to the initial domains or to surface defects. © 2004 American Institute of Physics. [DOI: 10.1063/1.1687272]

Certain compositions of doped perovskite manganites exhibit colossal magnetoresistance (CMR), and may be half metallic. In these CMR materials, the metal-insulator transition coincides with the magnetic transition. Experimentally, the magnetic and transport properties of CMR materials have been shown to be highly sensitive to lattice distortions both in thin film and bulk form. Many groups have shown that properties such as the Curie temperature resistivity, and magnetoresistance are extremely sensitive to chemical and hydrostatic pressure as well as epitaxial strain due to lattice mismatch with an underlying substrate.<sup>1,2</sup> Furthermore, geometrical confinement of epitaxial thin films into islands will change the strain state and thus affect the magnetism and transport.

Of particular interest has been the correlation of the magnetic domain state with the structure in optimally doped CMR thin film materials. These materials have the composition  $\text{La}_{0.7}\text{AE}_{0.3}\text{MnO}_3$ , where AE=alkaline earth. Unpatterned CMR films have been analyzed using magnetic force microscopy (MFM) at room temperature.<sup>3</sup> In differing strain states at low temperature, the domains were observed to pin to defects in the film.<sup>4</sup> More detailed imaging of bicrystal grain boundaries in thin films and measurement of their  $T_C$ 's found that those temperatures were higher at grain boundaries than the grain interiors.<sup>5</sup> Magneto-optical imaging has also been used to probe the local domain structure of CMR thin films.<sup>6</sup> This study found that the local magnetization is oriented out of the plane at bicrystal grain boundaries. Magnetic domain structure in these CMR films also gives rise to distinctive magnetotransport specifically attributed to the do-

main walls.<sup>7,8</sup> Moreover, it has been shown that ultrathin doped manganite films exhibit a more pronounced magnetoresistance effect than their thicker counterparts.<sup>7</sup> Sun *et al.* also reported that conductance linearly scales to zero at finite film thickness in CMR thin films grown on a variety of substrates.<sup>9</sup> Taken together, these results suggest that there is a surface or interface layer that has electronic properties very different from the rest of the film. Therefore the magnetic as well as the electronic properties of CMR thin films may not scale with thickness as one would expect. Previous work on  $\text{La}_{0.7}\text{Sr}_{0.3}\text{MnO}_3$  (LSMO) thin films patterned into island structures has shown that the nature of local magnetic structure in submicron islands of colossal magnetoresistive thin films does not differ dramatically from that of continuous films when the islands have low aspect ratios.<sup>10</sup> In these islands, the shape anisotropy as well as magnetostriction are the key factors that determine the evolution of domains and magnetization reversal.

In this paper, we present a more complete study of the magnetics of LSMO thin films, and corresponding patterned islands, with film thicknesses of 10–200 nm. This range of thicknesses includes the Matthews-Blakesley critical thickness of our epitaxial CMR films grown on  $\text{LaAlO}_3$  ( $\sim 40$  nm), below which the film should be under elastic strain without plastic deformation.<sup>11</sup> Moreover, the thinner films of this series may be dominated by a surface or interface related dead layer that has been deduced to be 5 nm for CMR films grown on  $\text{LaAlO}_3$  by Sun *et al.*<sup>9</sup>

We describe the orientation of the manganites in terms of the pseudocubic lattice parameters. For LSMO,  $a'_{\text{bulk}} = b'_{\text{bulk}}$

$=c'_{\text{bulk}}=3.87 \text{ \AA}$ . These lattice parameters are rotated  $45^\circ$  from the rhombohedral, nearly cubic lattice parameters  $a_{\text{bulk}} \approx b_{\text{bulk}} \approx c_{\text{bulk}} \approx 5.48 \text{ \AA}$ . The pseudocubic lattice parameters for  $\text{LaAlO}_3$  (LAO) are  $a'_{\text{bulk}} = b'_{\text{bulk}} = c'_{\text{bulk}} = 3.80 \text{ \AA}$ . LSMO films 10–200 nm thick were deposited epitaxially on (001)-oriented LAO substrates by pulsed laser deposition. A stoichiometric target of LSMO is ablated using a focused 248 nm KrF excimer laser. The substrates were held at  $700^\circ\text{C}$  in a 320 mTorr pure oxygen atmosphere. The lattice mismatch between LAO and LSMO places the films under  $\sim 2\%$  compressive strain. The films are compressively strained giving rise to a perpendicular magnetic anisotropy.  $2\theta$ - $\theta$  x-ray diffraction scans reveal epitaxial growth of the LSMO on LAO. Only the (001) families of peaks for LSMO and LAO are present in the scan. The measurement of the full width at half maximum for all of our films is limited by the resolution of the x-ray diffractometer and is  $<0.3^\circ$ . This implies that the films are of high crystalline quality. The islands were patterned from continuous films using standard photolithography techniques. The patterns are defined using an *I*-line stepper, then etched using an ion mill. Ion milling is somewhat problematic as it carbonizes the photoresist, however, it is necessary since the LSMO films are highly chemically resistant.

We have verified the composition and thickness of our films using Rutherford backscattering (RBS). RBS was performed on polycrystalline LSMO films that were grown on Si substrates in tandem with the samples grown on LAO. The samples on Si provide much better contrast in the RBS spectrum than the samples grown on LAO. Composition results are within 10% of the stoichiometry of the ablated target. The RBS measured thickness is accurate to within  $\approx 5\%$  of the actual film thickness. We also probed the surface morphology of our films and islands with atomic force microscopy. Though the resulting root mean square (rms) roughness of our unpatterned films slightly increases, on average, for thicker films, the dominant factors in determining the roughness are growth conditions. The unpatterned films ranging in thickness from 10–200 nm have RMS roughness ranging from 0.5–2.0 nm.

Using a superconducting quantum interference device magnetometer, we measured the saturation magnetization of our films at 5 K both in the in-plane and perpendicular directions. All of our films exhibit saturation magnetization values consistent with bulk values.<sup>12</sup> We found that  $T_C$  is suppressed as the film thickness decreases.  $T_C$  has been measured as low as 265 K for a 10 nm thick film. The suppression of  $T_C$  was also observed in the magnetization versus temperature and resistivity measurements. This agrees with previous observations that  $T_C$  increases as strain in the film is released.<sup>13–15</sup>

The compressive biaxial strain on the film due to the substrate gives rise to a perpendicular magnetic anisotropy. We investigated the magnetic structure of our films using MFM. Specifically we used magnetically coated tips magnetized in the perpendicular direction and scanned 20–50 nm above the surface of the film. Because of the high coercivity of our films and the low field produced by the tips, magnetization of our films is not a confounding factor. MFM

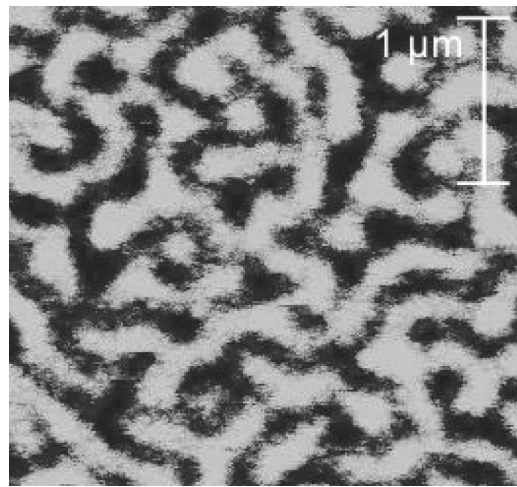


FIG. 1. A MFM image of an unpatterned film 53 nm thick after a 1 T magnetic field was applied in the perpendicular direction. The domains are 125 nm wide.

probes approximately an exchange length into the film,  $\approx 50 \text{ nm}$  for our films. MFM reveals stripe domains indicative of perpendicular anisotropy. Stripe domains form due to a competition between the exchange, magnetostatic, and magnetic anisotropy energies. In our case, the perpendicular anisotropy is large enough to overcome the magnetostatic energy and thus form stripes. MFM reveals domains of widths 125 nm in a 53 nm thick film, as shown in Fig. 1. The MFM studies of our unpatterned thin films show a square root dependence of the domain size with film thickness. This agrees with Kittel's basic scaling model.<sup>16</sup> MFM measurements performed after saturation in various in-plane and perpendicular directions reveal stripe domains parallel to the direction of the previously applied field—a result of the minimization of the associated Zeeman energy. Domain sizes, for patterned and unpatterned sets, appear to be similar with a slight suppression possible in the island samples (see Fig. 2). We are unable to see MFM images of the domain structure in films thinner than about 40 nm. Attempts by other researchers to image films below this threshold have

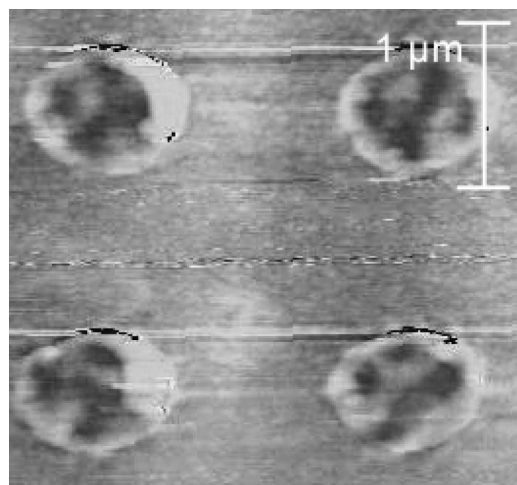


FIG. 2. A MFM image of the patterned version of the film in Fig. 1, after a 1 T magnetic field was applied in the perpendicular direction.

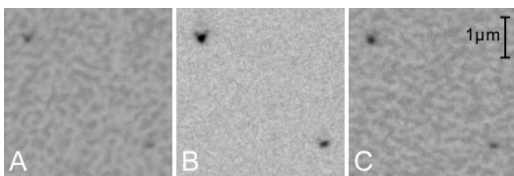


FIG. 3. PEEM images of the sample featured in Fig. 1. In view (a) the sample was at room temperature. In view (b) it was raised above  $T_C$ , and in view (c) it was cooled back to room temperature. Note how the domain structure retains no history between the two room temperature images.

met with little success.<sup>17</sup> This may be due to either the lower magnetization of the thinnest films reducing the interaction with the MFM tip or the dominance of shape anisotropy over strain anisotropy for ultrathin films.

Magnetic domain formation in our unpatterned thin films was also investigated using photoemission electron microscopy (PEEM). Additionally we extracted chemical and structural information from the PEEM studies by summing the left and right circularly polarized dichroism signals instead of taking the difference. *In situ* heating of our sample with a filament located behind the substrate allowed us to vary the temperature. Measurements were taken from room temperature to above 400 K, in excess of  $T_C$  (around 360 K). Soh *et al.* previously investigated the temperature dependence of the magnetic domain structure at artificial grain boundaries using MFM in CMR films with in-plane anisotropy, and observed an increase in  $T_C$  at these boundaries.<sup>5</sup> Our study, on the other hand, focuses on films with perpendicular anisotropy.

Below  $T_C$  the domains are clearly visible, disappearing as the temperature is increased through  $T_C$ . When the sample is cooled down the domains reform, but without any correlation to their previous structure. Comparing the surface morphology of the sample (deduced from the sum of the signals) to the magnetic domain structure (deduced from the difference of the signals), we do not see any correlation, implying that the magnetic domains are not pinning to defects in the unpatterned films. The surface morphology does not change as a function of temperature, as one would expect. In Fig. 3 domains about 125 nm in width disappear and reform in a 53 nm thick film as the sample is warmed then cooled through  $T_C$ . A similar effect was seen by Lu *et al.* in  $\text{La}_{0.65}\text{Ca}_{0.35}\text{MnO}_3$ , but in that study, as in the study by Biswas *et al.*, the domains were observed to pin to the film defects.<sup>18,4</sup> Previous MFM studies on LSMO have seen domain pinning in patterned island samples, suggesting that pinning is enhanced by patterning.<sup>10</sup>

The PEEM probes only the surface layer, as the electron escape depth is 2–5 nm. Therefore the scan can only detect a few unit cells into the sample, in contrast to MFM, which

probes an entire exchange length below the surface. The fact that we observe nearly identical stripe domain images with both PEEM and MFM suggests that the surface layer of the film is in the same magnetic state as the whole film. Therefore, the dead layer that some groups deduced from transport measurements of ultrathin films is most likely an interface layer and not a surface layer.<sup>9</sup>

In summary, we have grown LSMO thin films of 10–200 nm in thickness. Magnetic domains in our LSMO thin films thicker than 40 nm were observed with both MFM and PEEM. The domain structure detected by both techniques is very similar, implying that the domain state is the same for the film and the surface layer, and therefore that the previously observed dead layer is most likely an interface, not a surface, effect. We observed domain destruction and nucleation, as samples were heated and cooled through  $T_C$ . The domain nucleation occurred spontaneously across the entire film as it cooled through  $T_C$  with little pinning of domain walls.

The authors thank Kin Man Yu for taking some of the RBS data and Rajesh Chopdekar, Lisa Alldredge, and Jostein Grepstad for valuable discussions. This work was supported by the National Science Foundation (Grant No. DMR-0102621) and the David and Lucile Packard Foundation. In addition, this work made use of the facilities of the Cornell Center for Materials Research (Grant No. CCMR-MRSEC DMR-0079992) and the Cornell Nano-Scale Science and Technology Facility (Grant No. NSF ECS-9731293).

<sup>1</sup>K.K. Choi, T. Taniyama, and Y. Yamazaki, J. Appl. Phys. **90**, 6145 (2001).

<sup>2</sup>E.S. Vlahov, K.A. Nenkov, T.I. Donchev, and A.Y. Spasov, Vacuum **69**, 255 (2003).

<sup>3</sup>M.E. Hawley, G.W. Brown, and C. Kwon, Proc. Mater. Res. Soc. Science and Technology of Magnetic Oxides Symposium Materials Research Society **494**, 263 (1998).

<sup>4</sup>A. Biswas *et al.*, Phys. Rev. B **63**, 184424 (2001).

<sup>5</sup>Y.A. Soh, G. Aeppli, N.D. Mathur, and M.G. Blamire, Phys. Rev. B **63**, 020402 (2000).

<sup>6</sup>D.J. Miller, Y.K. Lin, V. Vlasko-Vlasov, and U. Welp, J. Appl. Phys. **87**, 6758 (2000).

<sup>7</sup>H.S. Wang and Qi Li, Appl. Phys. Lett. **73**, 2360 (1998).

<sup>8</sup>N.D. Mathur *et al.*, J. Appl. Phys. **86**, 6287 (1999).

<sup>9</sup>J.Z. Sun, D.W. Abraham, R.A. Rao, and C.B. Eom, Appl. Phys. Lett. **74**, 3017 (1999).

<sup>10</sup>Y. Wu, Y. Matsushita, and Y. Suzuki, Phys. Rev. B **64**, 220404 (2001).

<sup>11</sup>J.W. Matthews, A.E. Blakeslee, and S. Mader, Thin Solid Films **33**, 253 (1976).

<sup>12</sup>A. Urushibara *et al.*, Phys. Rev. B **51**, 14 103 (1995).

<sup>13</sup>A.J. Millis, T. Darling, and A. Migliori, J. Appl. Phys. **83**, 1588 (1998).

<sup>14</sup>Q. Gan *et al.*, Appl. Phys. Lett. **72**, 978 (1998).

<sup>15</sup>R.A. Rao *et al.*, J. Appl. Phys. **85**, 4794 (1999).

<sup>16</sup>C. Kittel, Phys. Rev. **70**, 965 (1946).

<sup>17</sup>C. Kwon *et al.*, J. Magn. Magn. Mater. **172**, 229 (1997).

<sup>18</sup>Q. Lu, C. Chen, and A. de Lozanne, Science **276**, 2006 (1997).